Mutation of the mouse Klotho gene leads to a syndrome resembling ageing

Article *in* Nature · December 1997

DOI: 10.1038/36285 · Source: PubMed

16 authors, including:

Yutaka Matsumura
Japanese Red Cross Saitama Hospital
41 PUBLICATIONS **5,899** CITATIONS
SEE PROFILE

Hiroshi Kawaguchi
Jhoban Hospital <Fukushima, Japan
532 PUBLICATIONS **36,663** CITATIONS
SEE PROFILE

Tatsuo Suga
Gunma University
67 PUBLICATIONS **6,051** CITATIONS
SEE PROFILE

Masahiko Kurabayashi
Gunma University
950 PUBLICATIONS **23,604** CITATIONS
SEE PROFILE

Mutation of the mouse *klotho* gene leads to a syndrome resembling ageing

Makoto Kuro-o*, Yutaka Matsumura*†, Hiroki Aizawa*†, Hiroshi Kawaguchi‡, Tatsuo Suga†, Toshihiro Utsugi†, Yoshio Ohyama†, Masahiko Kurabayashi†, Tadashi Kaname§, Eisuke Kume‖, Hitoshi Iwasaki‖, Akihiro Iida¶, Takako Shiraki-Iida*¶, Satoshi Nishikawa#, Ryozo Nagai†☆ & Yo-ichi Nabeshima*☆††

** Division of Molecular Genetics, National Institute of Neuroscience, NCNP, 4-1-1 Ogawahigashi, Kodaira, Tokyo 187, Japan*
† The 2nd Department of Internal Medicine, University of Gunma School of Medicine, 3-39-22, Showa, Maebashi, Gunma 371, Japan
‡ Department of Orthopaedic Surgery, Faculty of Medicine, University of Tokyo, 7-3-1 Hongo, Bunkyo, Tokyo 113, Japan
§ Institute of Molecular Embryology and Genetics, Kumamoto University School of Medicine, Kumakoto 862, Japan
‖ Lead Optimization Research Laboratory, Tanabe Seiyaku Co. Ltd, 2-2-50 Kawagishi, Toda, Saitama 335, Japan
¶ Tokyo Research Laboratories, Kyowa Hakko Kogyo Co. Ltd, 3-6-6 Asahimachi, Machidashi, Tokyo 194, Japan
 # Pharmaceutical Research Laboratories, Kyowa Hakko Kogyo Co. Ltd, 118 Shimotagari, Nagaizumi, Sunto, Shizuoka 411, Japan
☆ Core Research for Evolutional Science & Technology (CREST), JRDC and †† Institute for Molecular and Cellular Biology, Osaka University, 1-3 Yamada-oka, Suita, Osaka 565, Japan

A new gene, termed *klotho*, has been identified that is involved in the suppression of several ageing phenotypes. A defect in *klotho* gene expression in the mouse results in a syndrome that resembles human ageing, including a short lifespan, infertility, arteriosclerosis, skin atrophy, osteoporosis and emphysema. The gene encodes a membrane protein that shares sequence similarity with the β-glucosidase enzymes. The *klotho* gene product may function as part of a signalling pathway that regulates ageing *in vivo* and morbidity in age-related diseases.

Ageing can be defined as the age-related deterioration of physiological functions necessary for the survival and fertility of an organism[1]. Common age-related diseases linked to these functions include arteriosclerosis, cancer, dementia and osteoporosis. To determine how these diseases come about is central to understanding human ageing.

One approach to investigating the mechanism of human ageing is to find genes that determine inherited premature-ageing syndromes and cause rapid development of multiple age-related diseases early in life. Candidate genes for some of these syndromes have been identified by positional cloning[2–4] and found to encode a putative helicase that unwinds the DNA duplex and directly affects DNA replication and repair, explaining why patients acquire various gene mutations in their somatic cells[5]. From these findings, we concluded that the genetic mutations associated with premature ageing syndromes are mutation-causing mutations[6]. To determine whether accumulation of mutations can cause the development of multiple age-related diseases, it will be necessary to identify as many premature-ageing syndrome genes as possible and to find animal models of human ageing and identify their genetic features.

Here we describe a transgenic mouse with several age-related disorders caused by an insertional mutation of a transgene. Mice homozygous for the transgene show various phenotypes resembling those in patients with premature-ageing syndromes: arteriosclerosis, osteoporosis, age-related skin changes and ectopic calcifications, together with short lifespan and infertility. (We named this mutant *klotho*, for one of the Fates, the Greek goddess who spins the thread of life.) We have identified the gene linked to these ageing syndromes: it is not a helicase, but a new type of membrane protein. This indicates that the ageing phenotypes seen in the *klotho* mouse may be brought about by completely different mechanisms from those responsible for the premature-ageing syndromes.

Generation of the *klotho* mouse

Previously we reported salt-sensitive hypertension in transgenic mice that overexpress the rabbit type-I sodium–proton exchanger[7]. In that study, 28 independent transgenic mice were produced by a standard microinjection method; three of the mice expressed the exogenous transgene but the other 25 strains did not. Each of the transgenic mice that did not express the transgene was independently mated in an attempt to obtain mice homozygous for the transgene-inserted allele and each was examined to determine whether any phenotypes caused by the insertional mutation had appeared. One of these mice, now termed *klotho*, exhibited interesting phenotypes that resembled human ageing; these phenotypes only appeared in mice homozygous for the transgene. Penetrance of all phenotypes was 100%. Because *kl/kl* mice develop normally up to at least 2 weeks of age in both macroscopic and histological appearance, the phenotypes seen in *kl/kl* mice cannot simply be a result of incomplete development.

Cumulative genotyping of heterozygous crosses revealed that the manner of transgene transmission was consistent with mendelian inheritance, demonstrating that intra-uterine or perinatal death of *kl/kl* mice had not occurred. The genetic background of the original *kl* mouse was a mixture of C57BL/6J and C3H/J. However, the phenotypes were the same for mice whose genetic background was replaced by BALB/c after repetitive backcrossing for more than 12 generations.

Ageing phenotypes in *klotho* mice

Growth retardation and short lifespan. Up to 3 to 4 weeks of age, *kl/kl* mice grow normally and are indistinguishable from their +/+ or *kl*/+ littermates. At that time, *kl/kl* mice begin to show growth retardation (Figs 1a and 2b, c), gradually become inactive and marantic, and die prematurely at ~8–9 weeks of age. Their average lifespan is 60.7 days, with no *kl/kl* mouse ever surviving for longer than 100 days (Fig. 2a). The gross appearance of *kl/kl* mice was normal, except that they showed kyphosis (Fig. 1b). We were unable to specify the cause of death because each of the disorders described below is not in itself fatal.

Hypokinesis and gait disturbance. Open-field testing demonstrated that the spontaneous activity of *kl/kl* mice over 6 weeks of age was no more than 50% of that of control mice (Fig. 2d, e). Hind-paw footprint analysis revealed an abnormal walking pattern in *kl/kl* mice (Fig. 2f). Mean stride lengths corrected for base widths were significantly decreased compared with control mice, resembling the parkinsonian gait of the human aged[8]: altered function of the central nervous system may contribute to this hypokinesis and gait disturbance. Histological analysis of the central nervous system revealed that the number of Purkinje cells was decreased and that some of them had degenerated, but there were no other age-related changes such as brain atrophy, senile plaques or amyloid deposits in *kl/kl* mice.

Atrophy of genital organs and thymus. The external genital organs of *kl/kl* mice are atrophic and both sexes are incapable of mating (Fig. 1c, d). Macroscopic observation of *kl/kl* mice during dissection revealed atrophy of the testes, uterus and ovaries (Fig. 1e, f). The thymus was barely detectable in any *kl/kl* mice at 6–9 weeks old. This is not caused by a developmental defect: rather, it is a result of severe atrophy after normal development as the thymus was normal in size at earlier developmental stages. Atrophy of the thymus is widely observed during ageing of both humans and mice[9].

Arteriosclerosis. In the aorta, we observed extensive medial calcification (Fig. 3a). In middle-sized muscular arteries, not only medial calcification but also intimal thickening were seen (Fig. 3b). Small arteries in the kidney were also extensively calcified (Fig. 3c). Arteriosclerosis first appears around 4 weeks after birth and progresses gradually with age. The vascular changes seen in *kl/kl* mice are very similar to those in humans that are found in arteriosclerosis of the Mönckeberg type, common in human ageing[10].

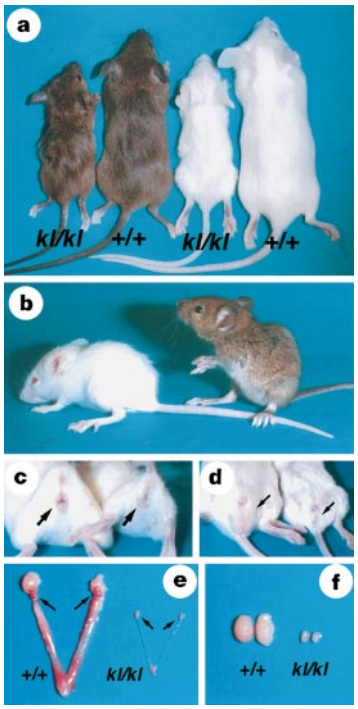

Figure 1 Macroscopic findings of *klotho* mice (8 weeks old). **a**, *kl/kl* mice with original (agouti) and with Balb/c background (albino) are shown with their +/+ littermates. **b**, Close-up of *kl/kl* mice. **c**, Female external genital organs. The vaginal opening (arrows) is open in +/+ mice (left), but closed in *kl/kl* mice (right). **d**, Male external genital organs. The scrotum (arrows) of *kl/kl* mice (right) is smaller than that of wild-type littermates (left). **e**, **f**, Female (**e**) and male (**f**) reproductive organs. Ovaries (arrows), uteri and testes are extremely atrophic in *kl/kl* mice.

Ectopic calcification. Ectopic calcification was evident in various organs of *kl/kl* mice as well as in arterial walls, including in the stomach (Fig. 7d), bronchial mucosa, alveolar cells, choroid plexuses, skin, testes and cardiac muscle. It also appears around 4 weeks after birth and progresses according to age. Overall, the distribution of ectopic calcification in *kl/kl* mice resembles that in natural human ageing[11].

Osteoporosis. In *kl/kl* mice, bone radiographs detected a generalized decrease in bone radiodensity, indicating the existence of osteopenia (Fig. 3d). This decrease in bone mineral density was particularly noticeable at the mid-portion of the long bones, where *kl/kl* mice had an approximately 20% lower density than control mice ($14.38 \pm 2.52\,mg\,cm^{-2}$ versus $19.19 \pm 0.74\,mg\,cm^{-2}$ in tibiae, and $21.40 \pm 1.79\,mg\,cm^{-2}$ versus $24.6 \pm 2.06\,mg\,cm^{-2}$ in femurs; mean $\pm$ s.d., $n = 5$), which is highly significant ($P < 0.01$). No sex differences were apparent. Histomorphometric analysis uncovered a decrease in the thickness of cortical bone. The number of osteoblasts and osteoclasts were decreased, suggesting a state of low turnover involving the formation and resorption of bone. All these findings bear a resemblance to senile osteoporosis in humans[12].

Skin atrophy. The hair of *kl/kl* mice was sparser than control mice. Histological examinations of the skin revealed a reduction in the number of hair follicles (Fig. 3e, f), another common feature of the aged[13]. There was also a reduction in dermal and epidermal thick-

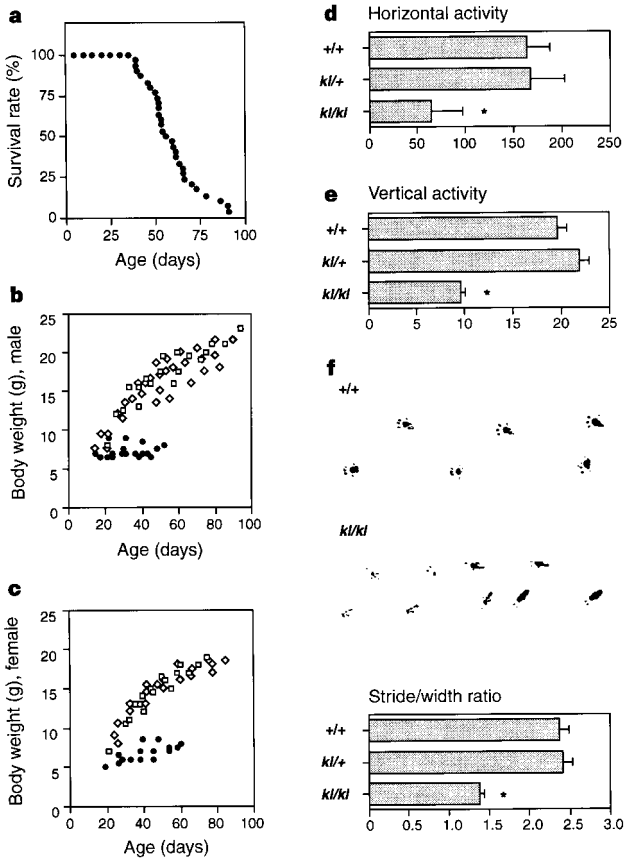

Figure 2 Short lifespan, growth retardation, and hypokinesis in *kl/kl* mice. **a**, Survival of *kl/kl* mice. The per cent survival *kl/kl* mice is plotted against age of the animals. **b**, **c**, Growth of male (**b**) and female (**c**) *klotho* mice. Body weight of *kl/kl* (circles), *kl*/+ (diamonds), and +/+ (squares) mice is plotted against age of the animals. **d**, **e**, Decrease in spontaneous horizontal (**d**) and vertical (**e**) activity detected by open-field test (see Methods). **f**, Hind-paw footprint test. Stride lengths corrected for the base widths (stride/width ratio) are decreased in *kl/kl* mice. Mean of the ten age- and sex-matched mice and s.d. (bars) were indicated. Asterisk, $P < 0.05$ versus +/+ and *kl*/+.

ness. The subcutaneous fat was barely detectable, and, in general, the skin displayed overall atrophy. These findings are very similar to those found in senile atrophoderma in humans[13].

Impaired maturation of gonadal cells. Both male and female *kl/kl* mice suffered impaired maturation of gonadal cells. In male *kl/kl* mice, the seminiferous tubules were extremely atrophic. Spermatocytes failed to differentiate beyond the pachytene stage and therefore sperm did not mature (Fig. 3g, h). In the ovary, we found only immature follicles; there were no mature secondary follicles, Graafian follicles or corpus luteum (Fig. 3i, j), indicating that neither male nor female gametocytes could accomplish the first meiotic division.

Emphysema. Histology of the lungs of *kl/kl* mice was characterized by enlargement of the air spaces distal to the terminal bronchiole, accompanied by destruction of the normal alveolar architecture (Fig. 3k, l). These changes are identical to those found in emphysema in humans, the incidence of which increases with age[14]. The respiratory function of *kl/kl* mice was consistent with emphysema (data not shown), but the oxygen content in arterial blood was almost normal when breathing room air.

Abnormalities in the pituitary gland. Immunohistochemistry of the pituitary glands of *kl/kl* mice confirmed that growth hormone (GH)-producing cells were smaller than those of control mice. The luteinizing-hormone- and follicle-stimulating-hormone-producing cells also seemed slightly atrophic (data not shown). The number of secretory granules in GH-producing cells was significantly decreased in *kl/kl* mice (Fig. 3m, n). These findings strongly suggest a defect in the signalling pathway for the appropriate production of pituitary hormones. Growth-hormone deficiency is known to contribute to the ageing process, resulting in growth retardation, reduced bone mass, reduced thymus weight, and reduced skin thickness[15], all of which were also seen in *kl/kl* mice.

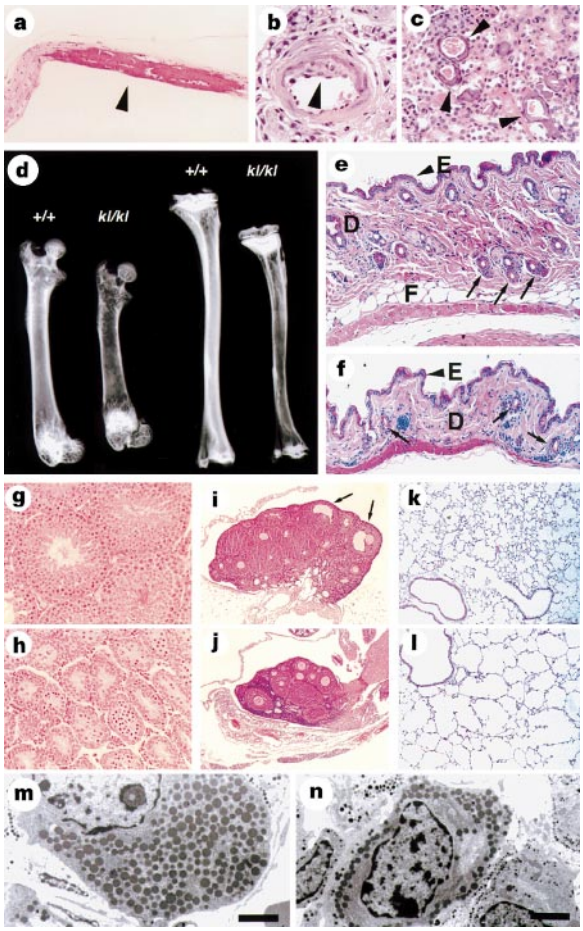

Figure 3 Histological analysis of *kl/kl* mice. **a**–**l**, Haematoxylin–eosin staining (not in **d**). **a**, Extensive medial calcification of the aorta (arrowhead, purple) in *kl/kl* mice. **b**, Intimal thickening in a muscular artery (arrowhead) in *kl/kl* mice. **c**, Calcification of the small arteries in kidney (arrowheads) in *kl/kl* mice. **d**, Bone radiographs of femurs (left two) and tibiae (right two). **e**, **f**, Skin of control (**e**) and *kl/kl* mice (**f**). Epidermal layer (E, arrowheads), dermal layer (D), subcutaneous fat layer (F), and hair follicles (arrows) are indicated. **g**, **h**, Testis of control (**g**) and *kl/kl* mice (**h**) at the same magnification. **i**, **j**, Ovary of control (**i**) and *kl/kl* mice (**j**). In control mice, there are mature secondary follicles (arrows). **k**, **l**, Lung of control (**k**) and *kl/kl* mice (**l**) observed in the same magnification. **m**, **n**, Electron micrograph of GH-producing cells in control (**m**) and *kl/kl* mice (**n**). Scale bar, 2 μm.

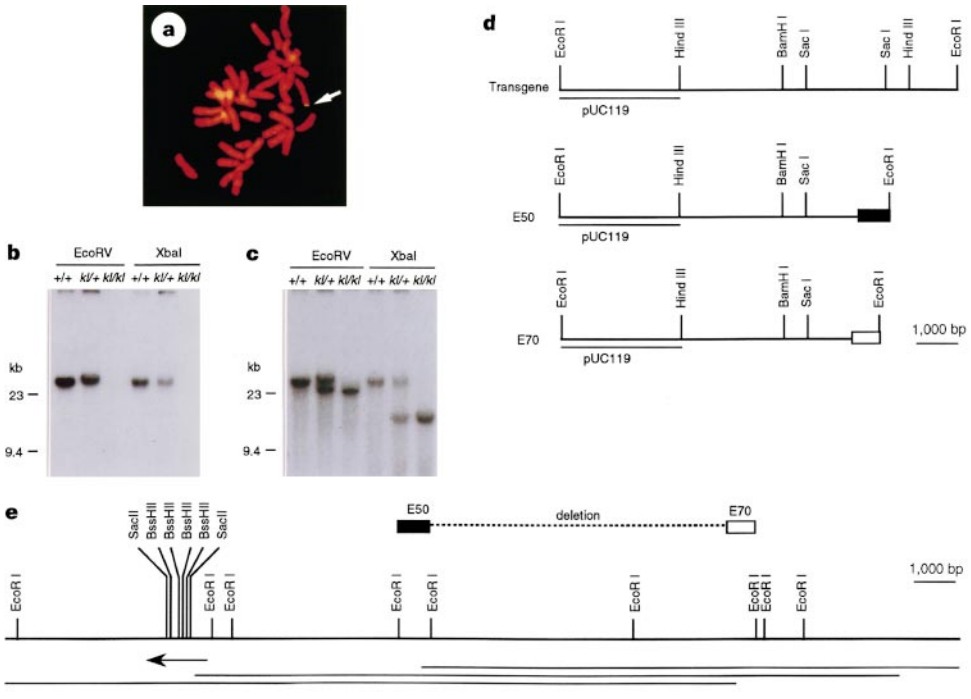

Figure 4 Identification of mouse *klotho* locus. **a**, Fluorescence *in situ* hybridization. The transgene insertion locus was determined as 5G3 (arrow). **b**, Southern blot analysis probed with the whole transgene. Genomic DNA from wild-type (+/+), heterozygous (*kl*/+) or homozygous (*kl/kl*) mice was digested with either *Eco*RV or *Xba*I. **c**, Southern blot analysis using the same filter as in **b**, using the E50-derived mouse genomic DNA fragment as a probe: the mutant (>50 kb) and wild-type alleles (25 kb by *Eco*RV digestin and 12 kb by *Xba*I digestion) were detected. **d**, Restriction maps of the transgene and the rescued plasmids. DNA originating from the mouse genome is indicated (E50, black box; E70, white box). **e**, Physical map of the mouse *kl* locus. Horizontal bars at the bottom indicate the overlapping phage clones isolated. The positions of E50- and E70-derived mouse genomic DNA are indicated as black and white boxes, respectively. The direction of *kl* gene transcription is indicated by an arrow.

Given that the GH production in *kl/kl* mice is impaired, it may affect the ageing phenotype.

Serum and blood data. A slight increase in calcium ($9.47 \pm 0.30\,mg\,dl^{-1}$ versus $10.64 \pm 1.07\,mg\,dl^{-1}$, mean ± s.d. of +/+ and *kl/kl* mice, respectively; $n = 12$) and phosphorus $8.54 \pm 1.34\,mg\,dl^{-1}$ versus $15.09 \pm 1.34\,mg\,dl^{-1}$) was observed, suggesting that these may contribute to ectopic calcification. Renal function seemed unaffected because creatinine levels were normal. *kl/kl* mice were hypoglycaemic ($231.5 \pm 22.6\,mg\,dl^{-1}$ versus $115.8 \pm 13.8\,mg\,dl^{-1}$), with decreased insulin in the pancreas, although it is not clear why. Peripheral blood analysis showed that the ratio of lymphocytes to leukocytes was decreased in *kl/kl* mice (61.3 ± 14.1% versus 34.5 ± 7.6%), consistent with atrophy of the thymus. Other data, including total protein, albumin, cholesterol and triglyceride levels, were normal in *kl/kl* mice. These results prove that the phenotypes of *kl/kl* mice are not derived from such disease conditions as malnutrition, abnormal lipid metabolism, or chronic renal failure.

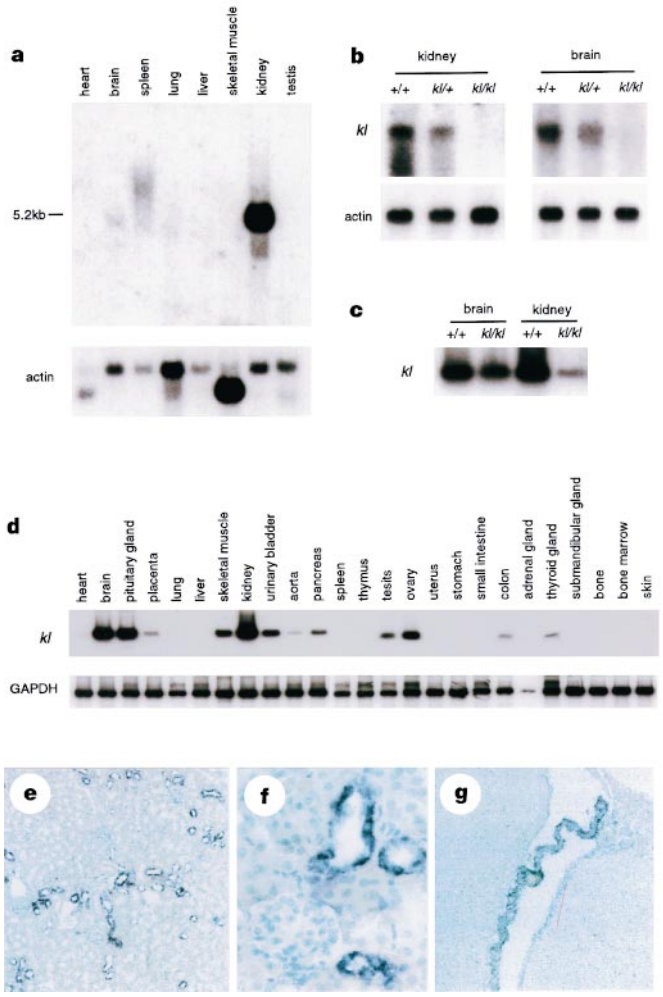

Figure 5 Expression of the mouse *klotho* gene. **a**, Northern blot analysis probed with the *Sac*II 450-bp genomic fragment from the *kl* locus (top panel) and human β-actin (bottom panel). Each lane contains 2 μg poly(A)$^+$ RNA (mouse MTN blot; Clontech). **b**, Northern blot analysis of poly(A)$^+$ RNA from kidney (left) and brain (right) of wild-type (+/+), heterozygous (*kl*/+) and homozygous (*kl/kl*) mice. **c**, RT–PCR analysis of mouse *kl* mRNA expression. PCR products were transferred onto a nylon membrane after electrophoresis and detected by a ^{32}P-labelled *kl* cDNA fragment. **d**, Top, expression of the *kl* gene in various tissues detected by RT–PCR, as in **c**; bottom, expression of mouse glyceraldehyde 3-phosphate dehydrogenase (GAPDH) detected by Control Amplimer Set (Clontech). **e**–**g**, *In situ* hybridization analysis of mouse *kl* mRNA expression in kidney (**e**, lower magnification; **f**, higher magnification) and brain (**g**) of control mice. Sense probe gave no signal (data not shown).

Cloning of the *klotho* gene

Approximately 20 copies of the transgene were integrated into the *kl/kl* mouse genome (data not shown). The chromosomal localization of the transgene insertion site was determined by the fluorescence *in situ* hybridization (FISH), using the whole transgene as a probe, which resulted in a single pair of symmetrical signals (Fig. 4a). In genomic Southern blot analysis using the whole transgene probe, only single bands were detected when genomic DNA was digested with restriction enzymes that do not cut the transgene (Fig. 4b). These results verify that multiple copies of the transgene were integrated in tandem at a single locus.

To generate the *klotho* mouse, the transgene was prepared by linearizing the transgene plasmid without removing the vector DNA (pUC119) (Fig. 4d). This allowed the convenient isolation of the DNA flanking the insertion locus by plasmid rescue (see Methods). Two kinds of plasmids (termed E50 and E70), each containing a short unique sequence of DNA that is not a part of the transgene, were recovered (Fig. 4d). Southern hybridization using these unique portions as probes indicated that they originated from the mouse genomic DNA flanking both ends of the transgene insertion site (Fig. 4c). A wild-type mouse genomic library was screened using the flanking DNA fragment as a probe. Three overlapping phage clones were isolated, covering about 25 kilobases (kb) of mouse genome (Fig. 4e). Both the E50 and E70 unique sequences were assigned to this region, separated by about 8 kb, indicating that the integration of the transgene produced a deletion of about 8 kb in the *kl* locus.

To identify exons in the *kl* locus, we determined the genomic sequence of the wild-type allele and analysed it with the exon-finding program GRAIL[16]. One of the GRAIL-predicted exons, located about 6 kb from the deletion site, contains multiple *Bss*HII (GCGCGC) and *Sac*II (CCGCGG) restriction sites, suggesting the existence of a CpG island (Fig. 4e). The 450-base-pair (bp) *Sac*II genomic fragment from this region was used as a probe for northern blot analysis and turned out to hybridize to an RNA fragment. The 5.2-kb transcript was detected predominantly in the kidney and faintly in the brain (Fig. 5a). Northern blot analysis of kidney and brain RNA from *kl/kl* mice showed that the *kl/kl* mouse is a null strain for this transcript (Fig. 5b). However, the more sensitive polymerase chain reaction with reverse transcription (RT–PCR) was able to detect its expression (Fig. 5c), indicating that the *kl* mutation was not a null but a severe hypomorph. We have determined the structure of the *kl* gene and found that it was in the 5′ upstream region that the deletion occurred in the mutated allele (data not shown). Therefore, the *kl* gene may be slightly transcribed in *kl/kl* mutants.

A mouse kidney cDNA library was screened with the 450-bp *Sac*II fragment, enabling the full-length cDNA to be isolated. The protein predicted from the cDNA sequence is 1,014 amino acids long and contains a putative signal sequence at its N terminus[17] and a single transmembrane domain near its C terminus, indicative of a new type-I membrane protein (Fig. 6a, b). We have confirmed by western blot analysis, indirect immunofluorescence, and fluorescent flow-cytometry that the recombinant KL protein is localized on cell surfaces when expressed in CHO cells (data not shown), which is consistent with the predicted KL protein structure.

The extracellular domain is composed of two internal repeats (termed mKL1 and mKL2), each about 450 amino acids long, which exhibit a weak similarity to each other (21% amino-acid identity). Each internal repeat shares homology with the β-glucosidases of both bacteria and plants and with a lactase–phlorizin hydrolase of mammals[18,19]; the amino-acid identity is between 20 and 40%. It remains to be determined whether the KL protein has β-glucosidase activity.

To isolate a human homologue of the *kl* gene, a human kidney

cDNA library was screened at a reduced stringency using the mouse 450-bp *Sac*II fragment. The isolated human *kl* cDNA encoded a protein 1,012 amino acids and showed 86% identity to the mouse KL protein (Fig. 6a). The chromosomal localization is 13q12, where no premature-ageing syndrome genes have been assigned.

Expression of the mouse *kl* gene

The RT–PCR technique detected low expression of the gene in the tissues other than the kidney and brain: the pituitary, placenta, skeletal muscle, urinary bladder, aorta, pancreas, testis, ovary, colon and thyroid gland (Fig. 5d). The transcript was not detected even by the RT–PCR in many other organs, including the stomach, lung, skin and bone, organs in which severe changes occurred in the mutants. During embryonic development up to 16 d *post-coitum*, expression of *kl* mRNA could not be detected by either northern blotting or *in situ* hybridization. However, northern blot analysis detected *kl* gene expression in the kidney of newborns (day 1). Expression of *kl* then occurs in the kidney through to adulthood (we have examined mice up to the age of 100 weeks).

To identify the cell types that express the *kl* gene, we did *in situ* hybridization with several cRNA probes. In kidney, the transcript appears only in distal convoluted tubules (Fig. 5e, f); in brain, the choroid plexus expresses *kl* (Fig. 5g). No signal was evident in organs that express the *kl* gene at levels only detectable by RT–PCR. In *kl/kl* mice, there was no signal in the kidney or in the brain.

Genetic rescue of *klotho* mice

To confirm that the candidate *kl* gene is responsible for all the phenotypes expressed by the mutant mice, we tested whether they could be rescued by exogenous expression of the candidate *kl* cDNA.

A total of 37 independent transgenic founder mice were produced by microinjection of a linearized construct that expresses mouse *kl* cDNA under the control of the human elongation factor EF-1α promoter, thought to be ubiquitously active at all developmental stages[20–22]. All the resulting transgenic mice were indistinguishable

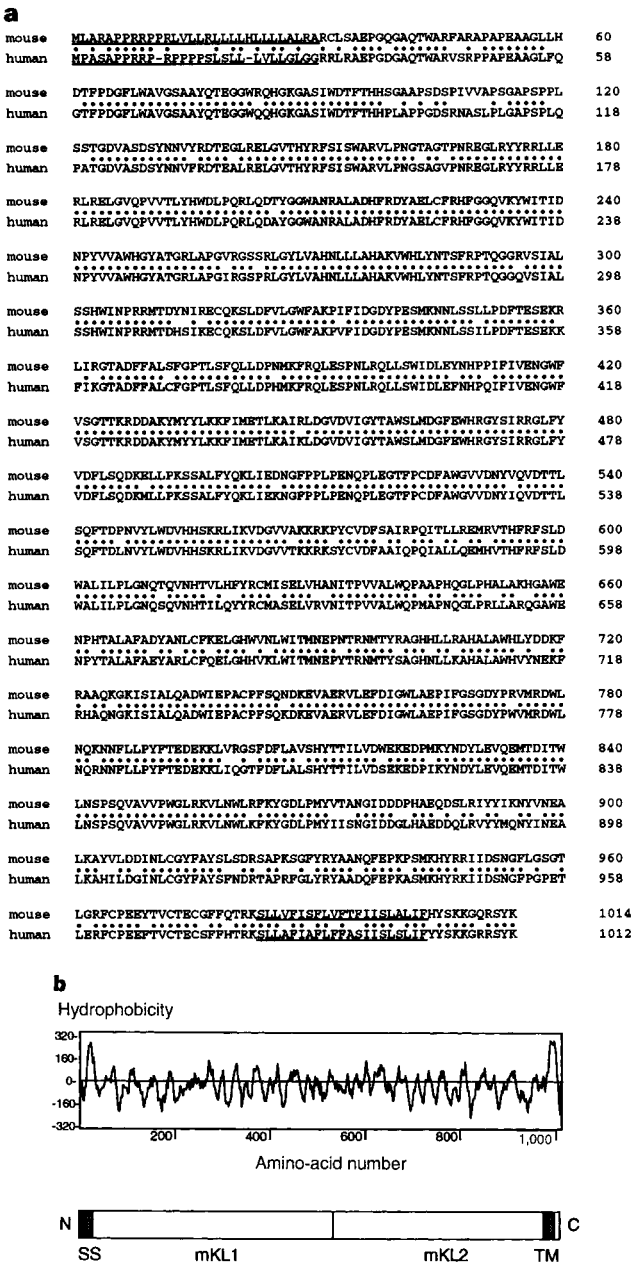

Figure 6 Amino-acid sequences and primary structure of mouse KL protein and its human homologue. **a**, Alignment of mouse and human amino-acid sequences. Identical amino acids are indicated by a dot. The predicted signal sequence (1–30 in mouse and 1–28 in human) and transmembrane domain (983–1,003 in mouse and 981–1,001 in human) are underlined. **b**, Top, Kyte–Doolittle hydrophobicity analysis of mouse KL protein (GeneWorks ver2.5; IntelliGenetics); bottom, predicted primary structure of mouse KL protein. The signal sequence (SS) and transmembrane domain (TM) are indicated by hatched boxes; the extracellular domain is composed of two internal repeats (mKL1 and mKL2) with weak homology.

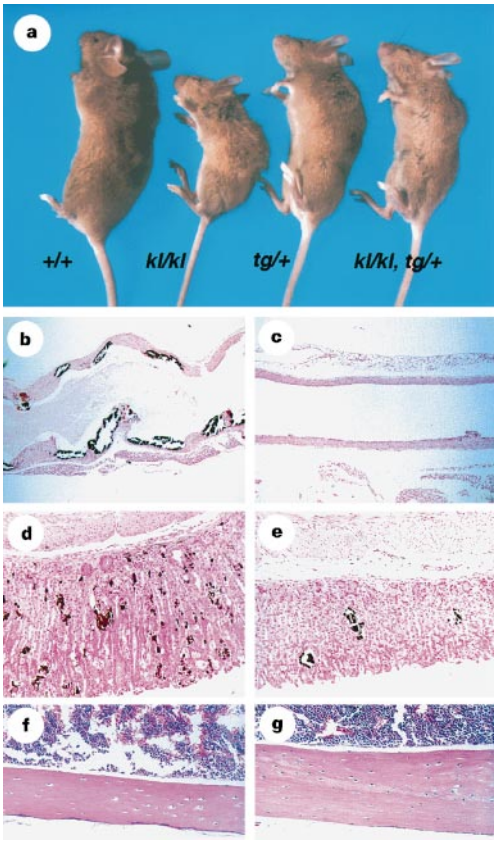

Figure 7 Rescue of the *klotho* mice by exogenous *kl* gene expression. **a**, Appearance of 7-week-old wild-type (+/+), *kl/kl*, *klotho* transgenic (*tg*/+) and rescued *kl/kl* (*kl/kl*, *tg*/+) mice. **b**, **c**, Aorta in 7-week-old *kl/kl* (**b**) and rescued *kl/kl* (**c**) mice. Von Kossa staining in which calcium is stained black. **d**, **e**, Stomach in 7-week-old *kl/kl* (**d**) and rescued *kl/kl* (**e**) mice. Von Kossa staining. Small calcium deposits persisted in the fundic gland cells (**e**), but were considerably less than those in *kl/kl* mice (**d**). **f**, **g**, Femur in 7-week-old *kl/kl* (**g**) mice. Haematoxylin–eosin staining is at the same magnification.

from wild-type mice. They were first mated with *kl*/+ mice to obtain transgenic mice carrying the heterozygous *kl* mutation in the F_1 generation; these mice were then backcrossed with *kl*/+ mice and, in the F_2 generation, transgenic mice carrying the *kl/kl* homozygous mutation were obtained and their phenotypes analysed.

Out of 37 transgenic mice, two independent strains, numbers 46 and 48, apparently rescued all of the macroscopic phenotypes observed in *kl/kl* mice. The *kl/kl* mice bearing the transgene were almost indistinguishable from their wild-type littermates in appearance and growth (Fig. 7a), and both males and females were fertile. The thymus and genital organs were also restored to nearly normal weights. The serum levels of calcium, phosphorus and glucose were restored to almost normal values (data not shown). Histological analysis revealed that various pathological findings were dramatically ameliorated or completely normal in the rescued *kl/kl* mice. Arteriosclerosis was markedly improved (Fig. 7b, c). Ectopic calcification was considerably less than in *kl/kl* mice (Fig. 7d, e). In the tibia and femur, the thickness of cortical bone was normal and osteopenia was improved (Fig. 7f, g). The other phenotypes, including emphysema, atrophy of GH-producing cells, impairment of gonadal cell maturation, and skin changes, were also eliminated (data not shown). Thus, all disorders observed in *kl/kl* mice were improved by exogenous *kl* gene expression according to macroscopic, histological and blood analyses. These results confirm that *kl* is the gene responsible for the mouse *klotho* phenotypes.

Exogenous *kl* gene expression was never detected by RNase protection assay in transgenic lines that failed to rescue *kl/kl* mice. In strain 46, the transgene was expressed in tissues such as the brain, lung, liver, testis and ovary, as expected. On the other hand, in strain 48, transgene expression was detected only in brain and testis (data not shown). Expression of the exogenous gene was never detected in kidney, where endogenous expression is predominant. In addition, all the systemic phenotypes of *kl/kl* mice were improved even when exogenous *kl* gene expression was limited to the brain and testis. These results can be interpreted in two ways: first, expression in the kidney may not be essential to the function of the *kl* gene; second, the pleiotropic effects of *kl* gene product may be cell non-autonomous.

Discussion

We have established a novel mouse autosomal recessive mutant, *klotho*, that exhibits multiple phenotypes very similar to those observed during human ageing. Although some common phenotypes seen in natural human ageing, such as the development of tumours or cataracts, are not seen in *kl/kl* mice, the *klotho* mouse can be regarded as a model of human premature ageing syndromes because the phenotypes displayed by them fulfil many of the pathophysiological criteria for human ageing[23]. No known laboratory mouse develops the syndrome observed in *kl/kl* mice, regardless of how long they live. Therefore, we should consider *kl/kl* mice as a model not for mouse ageing, but rather for human progeroid syndromes.

Senescence-accelerated mice (SAM) and their substrains have been developed for the study of human ageing and are known to exhibit ageing phenotypes, such as amyloidosis, osteoporosis and cataracts, among others[24]. The *klotho* mouse differs from SAM in several respects: first, the multiple ageing phenotypes in *kl/kl* mice are autosomal recessive and uninfluenced by genetic background, whereas the conditions of inheritance in SAM are more complex and have not yet been clarified; second, the multiple ageing phenotypes identified in *kl/kl* mice all appear in these mice, whereas the different phenotypes associated with SAM are distributed among the various SAM substrains; and last, the ageing phenotypes in *kl/kl* mice manifest much earlier than in SAM. We assume that multiple gene mutations are implicated in causing the phenotypes observed in SAM.

When possible functions are considered for the KL protein, it must be kept in mind that the *kl* gene is mainly expressed in specific cells and tissues. Some organs severely affected in *kl/kl* mice were not found to support *kl/kl* gene expression. In addition, the rescue experiment demonstrated that the exogenous *kl* gene expressed in limited organs could improve systemic ageing phenotypes in *kl/kl* mice. To explain these apparently non-cell-autonomous phenomena, it must be assumed that humoral factor(s) mediate the pleiotropic functions of the KL protein, at least in part. Our study indicates that ageing *in vitro* may be regulated through a humoral signalling pathway. Further investigation, including parabiosis experiments, will be needed to prove the existence of such humoral factor(s).

To our knowledge, the *klotho* mouse is the first laboratory animal model with multiple phenotypes resembling human ageing caused by a single gene mutation. Analysis of their pathophysiology will give clues not only to understanding the individual disease mechanisms but also the relationship between these mechanisms, essential to any discussion of human ageing. □

Methods

Histological examination. Ten male and 10 female *kl/kl* mice aged 6–9 weeks old, 4 male and 4 female *kl/kl* mice aged 4 weeks old, and 2 male and 4 female *kl/kl* mice aged 2 weeks old, were examined histologically together with age- and sex-matched *kl*/+ or +/+ mice. Organs were excised, fixed with 10% formaldehyde, embedded in paraffin, sectioned in 4-μm slices and stained with haematoxylin–eosin and von Kossa staining. The organs examined were liver, kidney, heart, lung, spleen, trachea, tongue, submundiblar gland, oesophagus, stomach, small intestine, large intestine, rectum, brain, cerebellum, eye, pituitary gland, adrenal gland, thyroid gland, parathyroid gland, genitalia, urinary bladder, femur, tibia, knee joint, ankle joint, thigh muscle, skin and aorta. The lungs were perfused through the trachea at a constant pressure of 20 cm H_2O with the fixative before fixing.

Behavioural analysis. Spontaneous locomotor activity was measured using a square arena (50 cm by 50 cm) with lattice lines at 5-cm intervals on its floor. A mouse was placed in the centre of the arena and horizontal activity was recorded by counting the total number of squares (5 cm by 5 cm) into which a mouse put its hind legs during 5 min. Vertical activity was recorded simultaneously by counting its rearing. The hind-paw footprint test has been described[25].

Fluorescence *in situ* hybridization (FISH). FISH was done as described previously[26]. Probes (the entire transgene for mouse and the cDNA fragment containing the entire open reading frame for human) were biotin-labelled by nick translation.

Southern and northern blotting. Southern and northern blotting were done according to standard methods[27]. For Southern blotting, genomic DNA prepared from liver was digested either by *Xba*I or *Eco*RV, which do not cut the transgene. After electrophoresis, DNA was transferred to a nylon membrane (Hybond-N+, Amersham). For northern blotting, poly(A)$^+$ RNA was prepared from various organs of +/+, *kl*/+ and *kl/kl* mice with oligo(dT) columns (Pharmacia), run on a denaturing formaldehyde/0.8% agarose gel, and blotted onto a Hybond N+ membrane according to the manufacturer's protocol. Probes were labelled with ^{32}P with random priming, using a commercially available kit (Amersham). A mouse multiple tissue northern blot was purchased from Clontech.

Plasmid rescue. Genomic DNA extracted from the liver of *kl/kl* mouse was completely digested with *Eco*RI and self-circularized with T4 DNA ligase (DNA Ligation System, TaKaRa) at the concentration of 10 μg ml^{-1}. To rescue plasmids from the possibly methylated transgene, the ligation mixture was transformed into competent cells defective in certain methylation-dependent restriction systems (XL1Blue MRF′, Stratagene) and plated on standard LB-ampicillin plates. All colonies were harvested and the rescued plasmids recovered by standard alkaline lysis.

Genomic and cDNA library screening. A mouse (129SVJ) genomic library, constructed on lambda FIX II (Stratagene), was used for cloning the *kl* locus. About 1×10^6 plaques were screened with a ^{32}P-labelled *Eco*RI–*Pvu*II 620-bp fragment from E50. Complementary DNAs were prepared from poly(A)$^+$ RNA of both an 8-week-old C57BL/6 male mouse kidney and human kidney

(Clontech). RNAs were primed with both oligo(dT)$_{12-18}$ and random hexamers simultaneously, then converted into cDNA using a commercially available kit (GIBCO BRL). cDNA libraries were constructed on lambda ZAP II (Stratagene) phage vector using Gigapack II Gold packaging extract (Stratagene). Approximately 9.0×10^5 primary plaques were obtained from both mouse and human kidney cDNA libraries.

RT–PCR. Poly(A)$^+$ RNA (500 ng) from various organs was reverse-transcribed with random hexamer (TaKaRa) and 5% of the reaction mixture was amplified with LA-*Taq* DNA polymerase (TaKaRa) using a specific primer pair for mouse *kl* cDNA (5′-CCTGGTCGACCATTTCAG-3′ and 5′-AGCACAAAGTCGACAG ACTTCTGGC-3′). Conditions for amplification were 30 cycles of 94 °C for 30 s, 56 °C for 30 s and 72 °C for 90 s.

***In situ* hybridization.** *In situ* hybridization was done using digoxigenin(DIG)-labelled antisense and sense riboprobes prepared by *in vitro* transcription of a mouse *kl* cDNA fragment (*Cla*I–*Xba*I, 356 bp) with DIG-UTP and either T3 or T7 RNA polymerase according to the manufacturer's protocol (Boehringer Mannheim). The hybridization signal was detected as a blue precipitate using alkaline phosphatase-labelled anti-DIG antibody and a substrate containing nitro-blue-tetrazoliumchloride (NBT)/X-phosphate. Nuclei were counterstained with methyl green.

Generation of transgenic mice for rescue. A 4.2-kb *Not*I fragment of the mouse *klotho* cDNA clone (the 5′ *Not*I site was derived from a polylinker of the λZAPII phage) containing the complete open reading frame was blunted and subcloned between the human elongation factor EF-1α promoter (including −580 bp upstream from exon 1, the first intron, and exon 2 truncated just 5′ of the ATG start codon) and the SV40 small-T poly(A) signal cassette. This plasmid was used for pronuclear microinjection after linearization by *Not*I digestion.

Received 17 June; accepted 17 September 1997.

1. Maser, E. J. in *Handbook of Physiology, 11: Aging* (ed. Masoro, E. J.) 3–24 (Oxford Univ. Press, New York, 1995).
2. Yu, C.-E. *et al*. Positional cloning of the Werner's syndrome gene. *Science* **272,** 258–262 (1996).
3. Ellis, N. A. *et al*. The Bloom's syndrome gene product is homologous to RecQ helicases. *Cell* **83,** 655–666 (1995).
4. Weeda, G. *et al*. A presumed DNA helicase encoded by ERCC-3 is involved in the human repair disorders xeroderma pigmentosum and Cockayne's syndrome. *Cell* **62,** 777–791 (1990).
5. Salk, D., Au, K., Hoehn, H. & Martin, G. M. Cytogenetics of Werner's syndrome cultured skin fibroblasts: variegated translocation mosaicism. *Cytogenet. Cell Genet.* **30,** 92–107 (1981).
6. Ellis, N. A. Mutation-causing mutations. *Nature* **381,** 110–111 (1996).
7. Kuro-o, M. *et al*. Salt-sensitive hypertension in transgenic mice overexpressing Na^+-proton exchanger. *Circ. Res.* **76,** 148–153 (1995).
8. Wolfson, L. & Katzman, R. in *Principles of Geriatric Neurology* (eds Katz, R. & Rowe, J. W.) 75–88 (Davis, Philadelphia, 1992).
9. Hausman, P. B. & Weksler, M. E. in *Handbook of the Biology of Aging* (eds Finch, C. E. & Schneider, E. L.) 414–432 (Van Nostrand Reinhold, New York, 1985).
10. Lansing, A. I. in *The Arterial Wall: Aging, Structure, and Chemistry* 136–160 (Williams & Wilkins, Baltimore, 1959).
11. Robbins, S. L., Angell, M. A. & Kumar, V. in *Basic Pathology* 3–27 (Igaku-shoin/Saunders, Tokyo, 1981).
12. Melton, L. J. & Riggs, B. L. in *Osteoporosis: Etiology, Diagnosis and Management* (eds Riggs, B. L. & Melton, L. J.) 155–179 (Raven, New York, 1988).
13. Chuttani, A. & Gilchrest, B. A. in *Handbook of Physiology, 11: Aging* (ed. Masoro, E. J.) 309–324 (Oxford Univ. Press, New York, 1995).
14. Sparrow, D. & Weiss, S. T. in *Handbook of Physiology, 11: Aging* (ed. Masoro, E. J.) 475–483 (Oxford Univ. Press, New York, 1995).
15. Corpas, E. S., Harman, M. & Blackman, M. R. Human growth hormone and human aging. *Endocr. Rev.* **14,** 20–39 (1993).
16. Uberbacher, E. C. & Mural, R. J. Locating protein-coding regions in human DNA sequences by a multiple sensor-neural network approach. *Proc. Natl Acad. Sci. USA* **88,** 11261–11265 (1991).
17. Heijne, G. A new method for predicting signal sequence cleavage sites. *Nucleic Acids Res.* **14,** 4683–4690 (1986).
18. Mantei, N. *et al*. Complete primary structure of human and rabbit lactase-phlorizin hydrolase: implications for biosynthesis, membrane anchoring and evolution of the enzyme. *EMBO J.* **7,** 2705–2713 (1988).
19. Grabnitz, F., Seiss, M., Rucknagel, K. P. & Staudenbauer, W. L. Structure of the β-glucosidase gene *bg/A* of *Clostridium thermocellum*. *Eur. J. Biochem.* **200,** 301–309 (1991).
20. Uetsuki, T., Nakao, A., Nagata, S. & Kaziro, Y. Isolation and characterization of the human chromosomal gene for polypeptide chain elongation factor-1α. *J. Biol. Chem.* **264,** 5791–5798 (1989).
21. Kim, D. W., Uetsuki, T., Kajiro, Y., Yamaguchi, N. & Sugano, S. Use of the human elongation factor 1α promoter as a versatile and efficient expression system. *Gene* **91,** 217–223 (1990).
22. Hanaoka, K., Hayasaka, M., Uetsuki, T., Fujisawa-Sehara, A. & Nabeshima, Y. A stable cellular marker for the analysis of mouse chimeras: the bacterial chloramphenicol acetyltransferase gene driven by the human elongation factor 1α promoter. *Differentiation* **48,** 183–189 (1991).
23. Martin, G. M. Genetic syndromes in man with potential relevance to the pathobiology of aging. *Birth Defects* **14,** 5–39 (1978).
24. Takeda, T., Hosokawa, M. & Higuchi, K. Senescence-accelerated mouse (SAM): a novel murine model of accelerated senescence. *L. Am. Geriatr. Soc.* **39,** 911–919 (1991).
25. Barlow, C. *et al*. *Atm*-deficient mice: a paradigm of ataxia telangiectasia. *Cell* **86,** 159–171 (1996).
26. Kaname, T. *et al*. Mapping basigin (BSG), a member of the immunoglobulin superfamily, to 19p13.3. *Cytogenet Cell Genet.* **64,** 195–197 (1993).
27. Sambrook, J., Fritsch, E. F. & Maniatis, T. *Molecular Cloning* (Cold Spring Harbor Laboratory Press, New York, 1989).

Acknowledgements. We thank E. Ozawa, T. Ishikawa, K. Hanaoka and I. Nonaka for earlier contributions to this work, T. Matsuzaki, S. Kameya and Y. Hiroi for maintaining mice, and H. Yamato and Y. Nagai for bone analyses.

Correspondence and requests for materials should be addressed to M.K. (e-mail: kuroo@ncnaxp.ncnp.go.jp) or Y.N. (e-mail: nabemr@imcb.osaka-u.ac.jp). The nucleotide sequence data will appear in the DDBJ, EMBL and GenBank nucleotide sequence databases under the accession numbers AB005141 and AB005142 for mouse and human mRNA for *klotho*, respectively.